



## **Application of Biomass-Based Nanomaterials in Energy**

Downloaded from: <https://research.chalmers.se>, 2025-12-08 23:26 UTC

Citation for the original published paper (version of record):

Yang, Z., Zhang, X., Zhang, J. et al (2023). Application of Biomass-Based Nanomaterials in Energy. Advanced Energy and Sustainability Research, 4(12). <http://dx.doi.org/10.1002/aesr.202300141>

N.B. When citing this work, cite the original published paper.

# Application of Biomass-Based Nanomaterials in Energy

Zhongwei Yang, Xiaoyu Zhang, Jian Zhang, Hong Liu,\* and Xin Yu\*

The utilization of biomass as a sustainable and renewable resource for nanomaterial synthesis has received considerable attention in recent years. Through the efficient utilization of biomass waste, opportunities for energy production, energy conversion, and the fabrication of nanomaterials can be maximized. The combination of biomass-based nanomaterials with additional nanomaterials makes the composite system have more remarkable performance, which further facilitates the transformation procedure of biomass-based nanomaterials for applications. This comprehensive review provides an overview of the preparation and applications of biomass-based nanomaterials. The preparation section covers a range of methods for synthesizing biomass-based nanomaterials, including biomass-based carbonaceous nanomaterials, biomass-based carbon nitride nanomaterials, nanomaterials derived from biomass templates, biomass-based nanomaterials as carriers, and the use of biomass for metal ion reduction. The applications section explores the diverse applications of biomass-based nanomaterials, such as hydrogen production, carbon dioxide reduction, batteries, and supercapacitors. The unique properties and advantages of biomass-based nanomaterials in each application are discussed. The conclusion summarizes the current progress and presents future perspectives for the development and utilization of biomass-based nanomaterials. This review emphasizes the potential of biomass as a valuable and sustainable source for nanomaterial synthesis, opening up promising opportunities in various fields.

## 1. Introduction

The distinctive characteristics exhibited by carbon nanomaterials have emerged as pivotal drivers of societal progress and technological advancements. However, the majority of carbon sources for synthesizing these nanomaterials primarily come from nonrenewable energy reserves, thus exacerbating the risks associated with fossil fuel depletion and environmental destruction.<sup>[1]</sup> Consequently, there is a pressing imperative to explore alternative carbon sources that are environmentally sustainable, economically feasible, and renewable. Biomass as an abundant and renewable carbon source represents an attractive solution to this challenge. Biomass is originated from agricultural, industrial, and forestry activities, represents a low-cost, widely available, environmentally benign, and renewable resource. The rational disposal of biomass as a by-product/biowaste from agriculture, industry, and forestry is an essential concern.<sup>[2]</sup> Owing to economic considerations, traditional approaches to biomass waste management have focused on mechanical and energy recovery meth-


ods.<sup>[3]</sup> However, recent advancements in nanotechnology have developed promising avenues for transforming various forms of biomass waste into high-value or low-hazard materials.<sup>[4]</sup> This transformation offers several advantages, including reduced recovery costs, minimized adverse environmental impacts, and enhanced recovery efficiency. Carbon nanomaterials conventionally derived from fossil fuels possess exceptional properties that render them highly versatile for diverse applications. Nonetheless, the reliance on fossil fuels for their production presents challenges such as resource scarcity and environmental degradation.<sup>[5]</sup> Utilizing biomass waste as a precursor for producing these valuable carbon nanomaterials not only mitigates dependence on fossil fuels but also addresses the ecological and environmental concerns associated with biomass waste management.<sup>[6]</sup>

Biomass, derived through the process of photosynthesis in the atmosphere, water, and land, constitutes an abundant and renewable carbon source in nature.<sup>[7]</sup> It encompasses a variety of organic compounds, including cellulose, starch, chitin, chitosan, pectin, lignin, vegetable oil, proteins, and so on.<sup>[8]</sup> Biomass energy, stored as chemical energy resulting from solar radiation, represents a paramount form of stored energy.<sup>[9]</sup> Its unparalleled ubiquity, abundance, and renewability distinguish it as a prime contender among various renewable energy sources. Globally,

Z. Yang, X. Zhang, H. Liu, X. Yu  
Institute for Advanced Interdisciplinary Research (iAIR)  
School of Chemistry and Chemical Engineering  
University of Jinan  
Jinan 250022, P. R. China  
E-mail: hongliu@sdu.edu.cn; ifc\_yux@ujn.edu.cn

J. Zhang  
Division of Systems and Synthetic Biology  
Department of Life Sciences  
Chalmers University of Technology  
41296 Göteborg, Sweden

H. Liu  
State Key Laboratory of Crystal Materials  
Shandong University  
Jinan 250100, P. R. China

 The ORCID identification number(s) for the author(s) of this article can be found under <https://doi.org/10.1002/aesr.202300141>.

© 2023 The Authors. Advanced Energy and Sustainability Research published by Wiley-VCH GmbH. This is an open access article under the terms of the Creative Commons Attribution License, which permits use, distribution and reproduction in any medium, provided the original work is properly cited.

DOI: 10.1002/aesr.202300141

more than 1.4 billion tons of biomass were produced annually, with a considerable portion comprising biomass waste generated by industrial, agricultural, and forestry practices. The efficient development and utilization of these natural biomass wastes transcend resource utilization and emerge as an urgent environmental imperative.<sup>[10]</sup> With the depletion of nonrenewable energy sources and the global temperature increasing, biomass waste has attracted widespread attention as an alternative energy source. Traditional biomass recycling methods were stuck in the primary stage of direct combustion and composting, which had the defects of poor value-added conversion rate and secondary pollution to the environment. Through the conversion and extraction of biomass waste to obtain higher value-added products can acquire better economic and environmental benefits to the maximum extent.<sup>[11]</sup> Since the 1970s, the efficient utilization and valorization of biomass waste have captivated widespread attention, resulting in significant strides and industrial-scale applications.<sup>[12]</sup>

The utilization of petroleum energy resources yields a considerable waste burden, which accumulates owing to the high recycling expenses. This perpetual accumulation of waste materials exerts a profound impact on soil, air, and water resources.<sup>[13]</sup> Utilizing the inherent properties of renewable biomass (e.g., plants, marine organisms, microorganisms, and biomass wastes), nanomaterials derived from biomass not only demonstrate favorable biocompatibility, environmental benignity, facile degradability, straightforward synthesis, substantial economic benefits and facile modifiability but also frequently manifest characteristics such as low thermal conductivity, low dielectric constant, and exceptional mechanical properties.<sup>[14]</sup> The further deployment of biomass-derived nanomaterials holds immense potential for accelerating nanomaterial fabrication and recycling processes, thereby mitigating the adverse environmental ramifications stemming from biomass waste. The distinctive properties arising from the conversion of biomass into nanomaterials could emerge as a pivotal domain and opportunity for the advancement of future green nanomaterials, applicable across various fields, including energy and beyond.<sup>[15]</sup> Presently, carbon nanomaterials derived from biomass have immense potential across different fields such as supercapacitors (SCs), fuel cells, sensing/bioimaging, photo/electrocatalysis, ecological restoration, and energy applications (Figure 1).

## 2. Preparation of Biomass-Based Nanomaterials

### 2.1. Biomass-Based Carbonaceous Nanomaterials

Carbon-rich biomass serves as a renewable and sustainable feedstock, and pyrolysis-based conversion of biomass holds significant promise in enhancing its economic viability.<sup>[16]</sup> The remarkable electron mobility, high thermal conductivity and permeability of 3D graphene films (3DGFs), and carbon nanotube fibers (CNTFs) have propelled their development in diverse domains, including energy storage, nanodevices, green chemistry, and catalysis.<sup>[17]</sup> Catalyst-assisted chemical vapor deposition (CVD) has emerged as a viable technique for synthesizing these nanomaterials. Nonetheless, this approach is less cost effective due to the extensive consumption of purified chemicals such

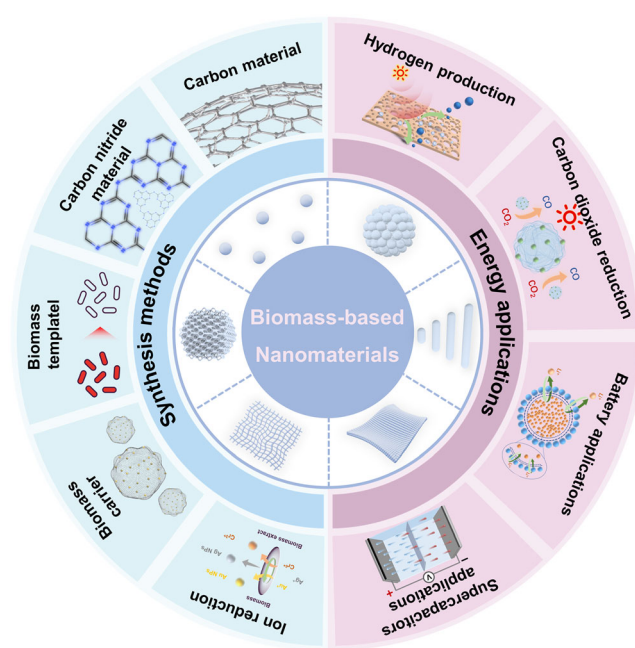


**Figure 1.** Schematic representation of the preparation method and application of biomass-based carbonaceous nanomaterials.

as hydrogen, methane, acetylene, or other precursors, as well as the prolonged deposition duration.

Exploiting low-cost carbon sources derived from biomass waste, such as lignin, cellulose, wheat straw, and sawdust, for the pyrolysis synthesis of 3DGFs and CNTFs represents a novel strategy to promote biomass conversion.<sup>[18]</sup> In fast pyrolysis, the biomass was pyrolyzed into biochar, bio-oil, and gas mixture at 800 °C. The gaseous product enters the gas-purification device, which contains alkali absorption solution and a molecular sieve, through the pipeline to obtain small-molecule gases. The purified gases were deposited onto the catalyst substrate and placed into the center of a CVD tube furnace at atmospheric pressure and a specific temperature. The fast-pyrolysis reactor in part 1 was heated to 800 °C. The feedstocks (powdered lignin, cellulose, and biomass wastes) were then fed to the reactor and decomposed into volatiles and carbon skeleton within 1–2 s. Following rapid pyrolysis, deposition, and etching steps under a strong reducing atmosphere, 3DGFs derived from different carbon sources exhibit comparable hollow three-dimensional network architectures composed of few-layer graphene sheets (Figure 2a,b), the ripples and wrinkles on the skeleton surface were retained. The SAED images exhibit multiple reflection spots in the hexagon, indicating the presence of graphene structures in the measurement area with rotational stacking faults. The structural layers of graphene were determined by HRTEM, and the curled edges of the film indicate that the 3DGF consisted of few-layered graphene sheets (<10 layers). Moreover, these biomass-derived 3DGFs possess lower mass density and higher electrical conductivity than most reported graphene aerogels, rendering them suitable for applications as electrodes in SCs, nanoscale electronic devices, and lightweight conductive materials. Additionally, the bio-oil obtained from

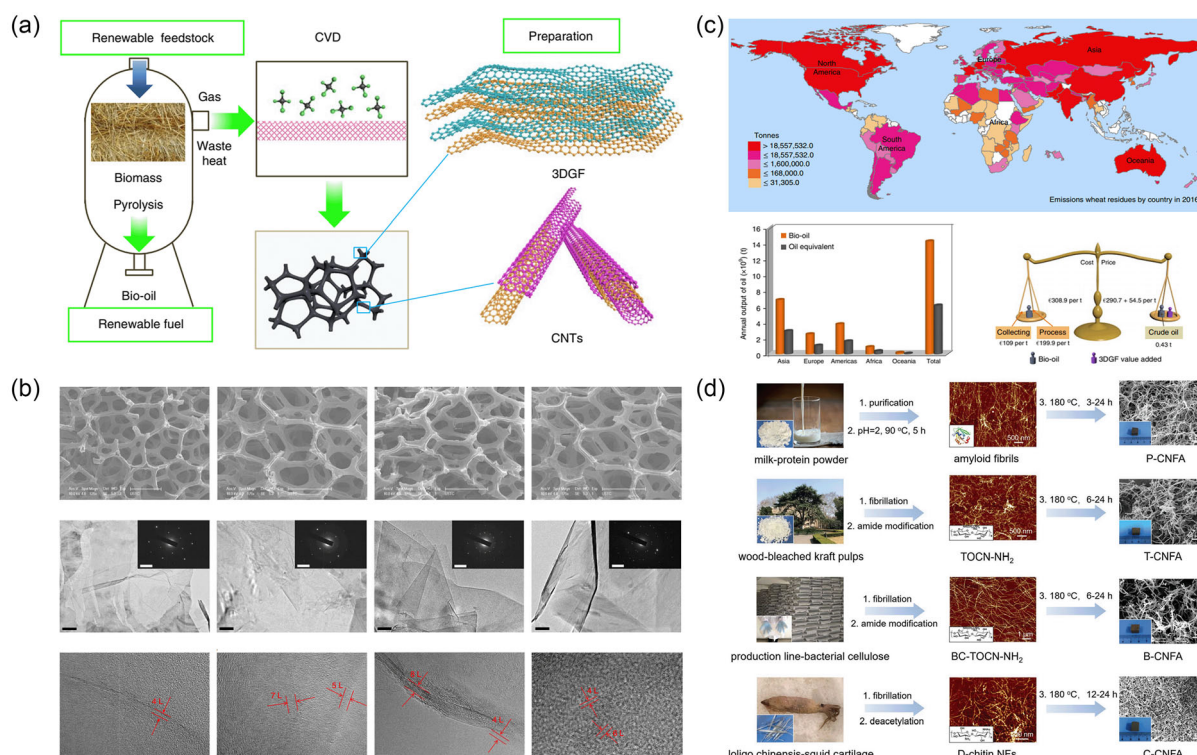


**Figure 2.** a) Schematic diagram of carbon nanomaterials prepared from biomass pyrolysis. b) Scanning electron microscope (SEM), transmission electron microscope (TEM), and high-resolution TEM (HRTEM) images of 3DGFs. c) Graph of biomass reserves and cost price. Reproduced with permission.<sup>[18]</sup> Copyright 2020, Springer Nature. d) Schematic of the process of preparing carbon nanofiber aerogels from different biomass precursors. Reproduced with permission.<sup>[23]</sup> Copyright 2022, Wiley-VCH.

rapid pyrolysis of grain biomass waste can effectively mitigate reliance on petroleum-based energy sources (Figure 2c). Compared to conventional CVD processes, this expedited pyrolysis synthesis route minimizes the impact on human health, ecological well-being, and global warming, thereby opening up new avenues for sustainable and safe production of high-value carbon-based nanomaterials.

Three-dimensional interconnected porous architectures endow aerogel materials with low density, large specific surface area, superior mass transfer properties, and low thermal conductivity, rendering them highly attractive for applications in energy storage, electrocatalysis, and other energy-related domains.<sup>[19]</sup> Conventional aerogels, typified by silica-based inorganic aerogels and organic aerogels like polybenzene dicarboxylate, consist of cross-linked primary nanoparticles (NPs), impeding precise microstructural control.<sup>[20]</sup> Recent efforts have explored the assembly of aerogels using NPs of varying sizes, aiming to address microscale manipulation. However, these methods suffer from complexity and limited economic efficiency.<sup>[21]</sup>

Currently, researchers are focusing on the development of superelastic structures utilizing carbonaceous aerogels derived from wood or bacterial cellulose.<sup>[22]</sup> A promising approach for fabricating carbonaceous nanofiber aerogels entails template-directed hydrothermal carbonization of biomass nanofibers, including cellulose, chitin,  $\beta$ -chitin and proteins (Figure 2d).<sup>[23]</sup> For them, all of prepared nanofibers contain a

large number of carboxyl groups, while there are also a large number of amino groups on the surface of protein nanofibers, which have been proved to be able to promote the nucleation growth of hydrothermal carbonaceous layers. Therefore, cellulose nanofibers and chitin nanofibers were surface aminated before use. Finally, uniform carbonaceous nanofibers were also obtained by using amino-functionalized nanofibrils and partially deacetylated chitin nanofibers as templates for directing hydrothermal carbonization process. In comparison to traditional biopolymer-based aerogels, carbonaceous nanofiber aerogels synthesized through this method exhibit remarkable recoverability, mechanical strength and surface functionality. The functional groups present on the aerogel's surface facilitate nucleation and growth of carbonaceous layers during the hydrothermal process. This sustainable synthesis technique, with its distinctive structure, unlocks novel possibilities for advancing the application and transformation of biopolymer aerogels.

## 2.2. Biomass-Based Carbon Nitride Nanomaterials

Doping carbon-based nanomaterials with heteroatoms have emerged as a promising avenue for the development of innovative catalysts, characterized by their low cost, facile synthesis, high surface area, tunable morphology, and excellent stability. Heteroatom-doped carbon-based nanomaterials have found wide-ranging applications in catalyst supports, sensors, fuel cells,



SCs, and various other fields.<sup>[24]</sup> Leveraging abundant and economically viable renewable resources for the pyrolysis synthesis of nitrogen-doped carbon nanomaterials represent an ideal preparation strategy. Silk, predominantly composed of hydrophobic fibroin proteins, serves as an environmentally friendly protein polymer. The coexistence of sericin and fibroin in silk provides a nitrogen source for the pyrolytic synthesis of nitrogen-doped carbon (Figure 3a). By utilizing natural silk cocoons as the carbon–nitrogen precursor, monofilament fibers consist of two parallel fibroin fibers that are adhered by hydrophilic sericin (Figure 3b). At molecular scale, silk fibroin comprises primarily hydrogen-bonded  $\beta$ -sheet crystallites embedded in a less-ordered  $\alpha$ -helix domain, leading to the exceptional strength and toughness of silk fibers. Under high-temperature heat treatment in the presence of KOH, as an active agent, the adjacent amide bonded protein chains can transform to aligned porous polyaromatic carbon structures (NC) due to intermolecular dehydration.<sup>[25]</sup> There are many small pores randomly distributed across the surfaces. These pores derived from the thermal treatment process in the presence of KOH in which small molecule gases released and left spaces in the NC support. The thermal pyrolysis of silk cocoons for the synthesis of nitrogen-doped carbon nanomaterials adheres to the principles of green chemistry, offering a fresh avenue for the utilization of biomass-derived nitrogen-doped carbon nanomaterials in the realm of catalysis.

In light of the escalating global energy and environmental challenges, the development of environmentally friendly and renewable energy sources has gained paramount importance. Metal-air batteries have emerged as promising solutions due to their high energy density and low emissions. However, their practical application is hindered by the sluggish kinetics of the oxygen reduction reaction (ORR) at the cathode.<sup>[26]</sup> Most reported ORR catalysts are derived from complex and costly organic

monomers, posing risks of environmental pollution.<sup>[27]</sup> In this context, the utilization of biomass waste for the preparation of carbon-based nanomaterials offers a compelling alternative, combining excellent stability, environmental friendliness, and the presence of multiple heteroatoms and unique coordination structures. These carbon-based materials present themselves as highly promising electrocatalysts for ORR applications.<sup>[28]</sup> Watermelon peel carbon (WPC) was obtained by precarbonizing the dried watermelon peel to remove partial hydroxyl groups and volatiles on the surface of the biomass, followed by carbonization under argon environment. Second, WPC was activated by KOH to obtain watermelon peel activated carbon (WPAC). Finally, WPAC was treated with urea to gain the watermelon peel-derived nitrogen-doped hierarchically porous carbon sample (N-WPAC) (Figure 3c).<sup>[29]</sup> The KOH activation process facilitates the construction of a well-defined porous structure, while the subsequent urea post-treatment further refines it into a layered porous structure, resulting in the formation of N-WPAC (Figure 3d). Remarkably, N-WPAC exhibits superior stability compared to conventional Pt/C catalysts and demonstrates excellent ORR activity, thereby providing a simple and effective pathway for the preparation of high-performance nonmetal catalysts using biomass waste as a valuable resource.

### 2.3. Nanomaterials Made From Biomass Templates

In recent years, there has been significant progress in the synthesis of nanomaterials with diverse morphologies, with template methods emerging as stable and effective approaches. Notably, natural microorganisms with diverse three-dimensional geometric shapes have proven valuable as mineralization templates for synthesizing highly dispersed structures such as rods, spheres, and hollow shells.<sup>[30]</sup> Leveraging these biological

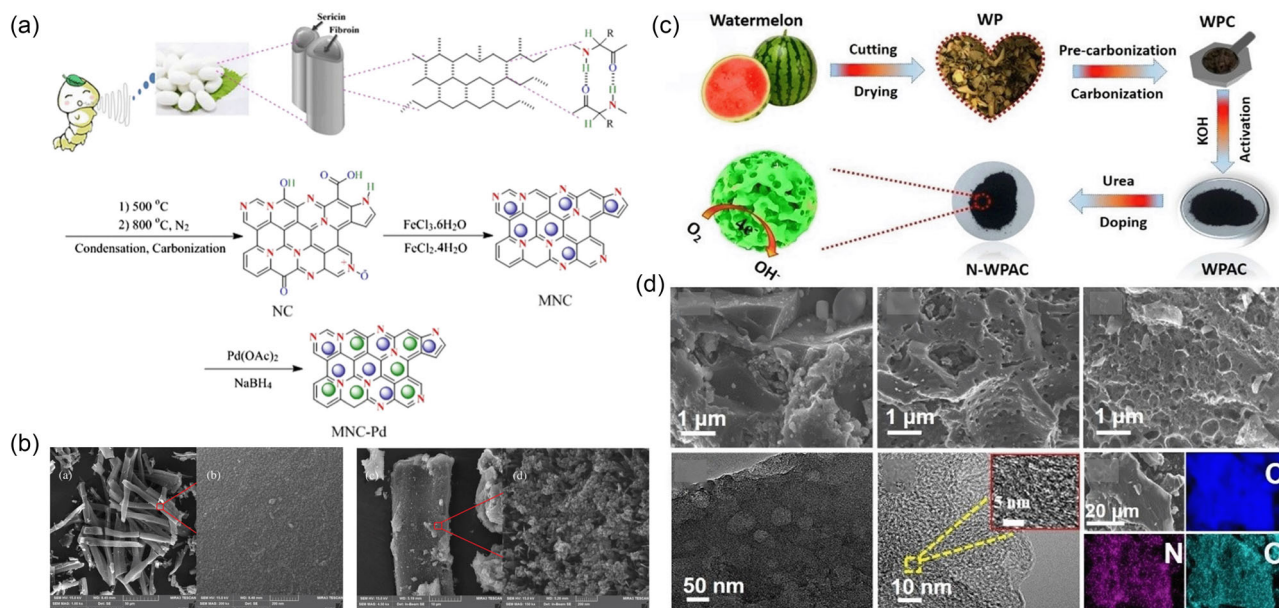


**Figure 3.** a) Schematic diagram of carbon nitride prepared from silk. b) SEM image of carbon nitride and carbon nitride loaded with functional components. Reproduced with permission.<sup>[25]</sup> Copyright 2021, Wiley-VCH. c) Schematic diagram of the synthesis of N-WPAC. d) SEM, TEM, and EDX elemental maps of N-WPAC. Reproduced with permission.<sup>[29]</sup> Copyright 2021, Wiley-VCH.

templates offers promising prospects for novel synthesis strategies, leveraging their varied morphology, uniform size, excellent solvent stability, and abundant surface functionality. Among these templates, *Escherichia coli* (*E. coli*) strains, which are harmless and widely distributed in the environment, food, and animal intestines, have been employed as biological templates for the fabrication of  $\text{TiO}_2/\text{Au}/\text{TiO}_2$  nanostructures, showcasing their powerful potential as surface plasmon resonance (SPR) photocatalysts assisted by whispering gallery mode (WGM) resonance (Figure 4a).<sup>[31]</sup> *E. coli* plays a dual role in reducing Au ions to Au NPs and guiding the formation of microcapsules exhibiting WGM properties. First,  $\text{Au}^{3+}$  aqueous solution was mixed with the culture solution containing *E. coli*. Au ions were first trapped on the cell wall by electrostatic interactions, which were subsequently reduced by protein/enzyme on the cell wall or with bacterial metabolites to form Au NPs attached on the bacteria surface. Finally, the *E. coli*/Au/ $\text{TiO}_2$  composite was calcined under an air atmosphere to remove *E. coli* and obtain an  $\text{E-TiO}_2/\text{Au}/\text{TiO}_2$  heterostructure (Figure 4b). The resulting photocatalysts exhibit excellent photocatalytic performance, with the recovery of precious metals offering significant economic and environmental benefits. This biofabrication method offers a promising bioprocess for the preparation of photocatalytic nanomaterials, demonstrating the potential of harnessing biological templates in nanomaterial synthesis.

Manganese oxides offer great potential as anode materials for lithium-ion batteries due to their cost-effectiveness and environmental friendliness. However, their lower conductivity compared to other metal oxides has limited their exploration in this field. To address this, researchers have successfully utilized *Bacillus sphaericus* as a template to selectively synthesize manganese

oxides with hollow rod-like nanostructures by incorporating  $\text{MnCl}_2 \cdot 4\text{H}_2\text{O}$  and  $\text{NaBH}_4$  for reflux stirring (Figure 4c).<sup>[32]</sup> The resulting manganese oxides exhibit single crystals or small clusters with a diameter of approximately 2–5 nm, uniformly attached to the bacterial template. Subsequent calcination removes the template, yielding manganese oxides with a hollow nanostructure (Figure 4d). Remarkably, these manganese oxide nanomaterials not only inherit the one-dimensional rod-like structure from the bacterial template but also possess a high specific surface area. Even after multiple cycles, the manganese oxide nanomaterials synthesized in this manner maintain a high reversible capacity, demonstrating their potential for advancing the application of manganese-based materials in the field of battery anode materials. This innovative approach paves the way for the development of high-performance manganese oxide-based electrodes in lithium-ion batteries.

#### 2.4. Biomass-Based Nanomaterials as Carriers

Compared with the procedure of removing the biomass template, the utilization of biomass nanomaterials as carriers provides enhanced exploitation of the inherent properties of biomass. Biomass-based nanomaterial carriers possess a variety of characteristics such as facilitating carrier deposition, reducing carrier loss, enlarging the active area of the carrier, strengthening the physicochemical properties of the composite system, and accelerating the rate of interfacial mass transfer. Cellulose, a key component of biomass, has garnered significant attention in various fields such as flexible electronic devices, dielectric layers, and derived carbon materials due to its abundant reserves,

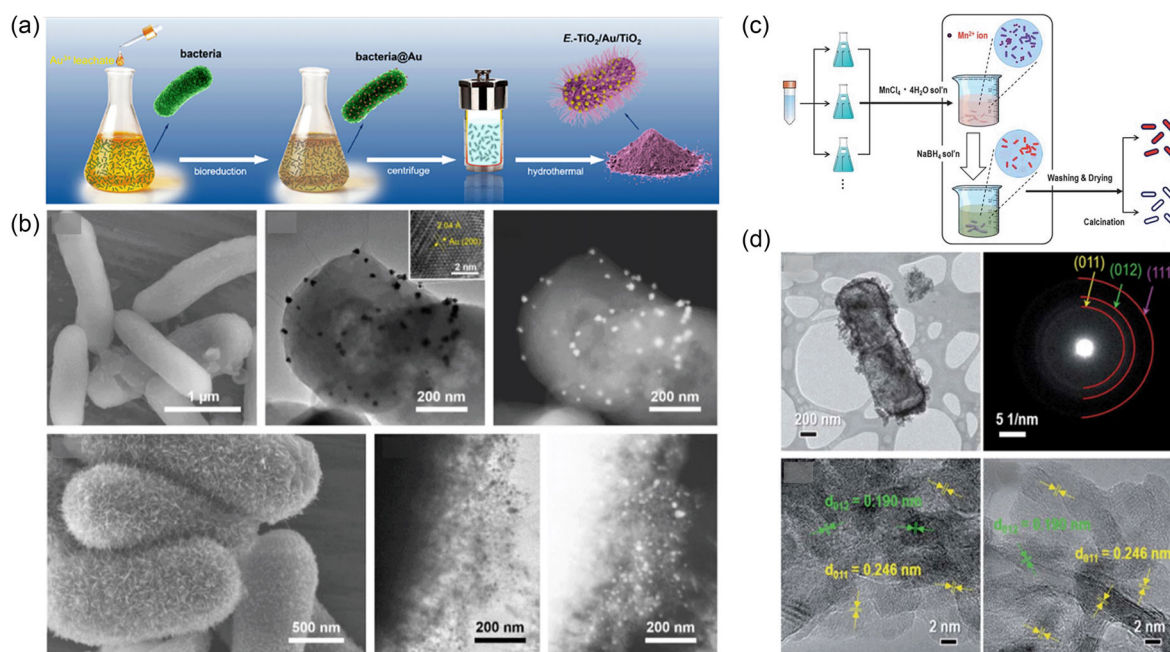


**Figure 4.** a) Schematic of the synthesis process of  $\text{TiO}_2/\text{Au}/\text{TiO}_2$  heterostructures. b) SEM and TEM images of *E. coli* and the  $\text{TiO}_2/\text{Au}/\text{TiO}_2$  heterostructures. Reproduced with permission.<sup>[31]</sup> Copyright 2020, American Chemical Society. c) Schematic representation of the synthesis process of bacterial templates of manganese oxide nanostructures. d) TEM and HRTEM images of bacterial/manganese oxide composite nanorods. Reproduced with permission.<sup>[32]</sup> Copyright 2011, Royal Society of Chemistry.

cost-effectiveness, biodegradability, and exceptional mechanical properties.<sup>[33]</sup> At the nanoscale, cellulose often exhibits enhanced performance, and its combination with conductive polymers, metal oxides, metal hydroxides, and carbon nanomaterials enables the formation of flexible conductive substrates suitable for solid-state supercapacitor assembly.<sup>[34]</sup> However, the practical application of cellulose-based nanomaterials is impeded by material aggregation and the degradation of mechanical and optoelectronic properties induced by the reaction system with water.<sup>[35]</sup> Thus, the development of efficient strategies to disperse nanomaterials is crucial for advancing the application of nanocellulose composite materials in energy storage devices. Deep eutectic solvents (DES), known for their green nature, biocompatibility, high stability, biodegradability, and material dispersion capabilities, offer a viable solution.<sup>[36]</sup> Leveraging DES for the one-step preparation of nanocellulose/reduced graphene oxide (CNF/rGO) film electrodes represents a simple and effective strategy to produce functional nanocellulose composite materials.<sup>[37]</sup> The resulting CNFs film exhibits an interwoven fiber structure with irregular cross-sections. Mix CNFs and graphene oxide (GO) sheet suspensions with DES and stir to obtain a homogeneous solution. The homogeneous solution was obtained by mixing CNFs and GO sheet suspension with DES and stirring. Subsequently, the GO content was minimized by the use of L-ascorbic acid (VC), covered on polyvinylidene fluoride (PVDF) after water bath treatment, and dried to obtain conductive composite films. Upon loading rGO nanosheets, the gaps between CNFs are filled, and the rGO effectively covers the film's surface, rendering the composite film more compact (Figure 5a,b). The layered structure of the composite film, akin to other cellulose materials, allows for increased interlayer spacing with higher CNFs content, facilitating enhanced contact between the electrode and the electrolyte. This, in turn, boosts the specific capacitance and stability of the electrode. Moreover, increasing the rGO content further enhances the flatness, thickness, and mechanical properties of the composite material. The resulting composite film exhibits remarkable flexibility, high conductivity, and exceptional mechanical properties, providing valuable insights for the design of functional nanocellulose composite materials. This work highlights the potential for utilizing nanocellulose composite materials in energy storage applications.

Carbon-based nanomaterials have emerged as exceptional catalyst supports in the field of catalysis, driving extensive research and applications. An effective catalyst support necessitates a large specific surface area to accommodate ample active sites for uniform catalyst loading.<sup>[38]</sup> While templating methods enable precise control over the pore size of carbon materials, they often involve high temperatures or chemical etching to remove the templates, resulting in energy consumption and environmental hazards.<sup>[39]</sup> To address these challenges, researchers have explored the use of four distinct biomass carbon precursors, namely bamboo, cotton, cork, and hardwood, for the preparation of porous carbons. These biomass-derived materials exhibit unique mesoporous structures and large specific surface areas, rendering them highly promising as catalyst supports (Figure 5c).<sup>[40]</sup> The chemical composition and surface functional groups of the carbon supports influence the nucleation and growth of catalysts, while the porous structure impacts the interfacial mass transfer between substrates and products. Leveraging

the tubular cell structure of natural plant fibers, the carbon precursors obtained from biomass undergo carbonization and oxidation processes, yielding micrometer-sized pores in the resulting carbon materials, which is derived from the tubular cell structure of natural plants. C<sub>Bamboo</sub> and C<sub>Maple</sub> remain their closely packed tube array structure, while C<sub>spruce-pine-fir</sub> shows separated tube cells that is attributed to the degradation of adhesive lignin between cells. C<sub>Cotton</sub> remained its fabric feature and microscopic hollow tube structure after the carbonization and oxidation processes. Focusing on the surface, uniform porous structures penetrating through the cell wall can be observed indicating the oxidation process not only generates pores at surface but also inner structure of carbon. The nucleation and growth processes of Ag NPs catalysts on the four types of biomass-derived carbon nanomaterials demonstrate variations attributed to differences in surface active groups and ions (Figure 5d). Furthermore, increasing the oxidation temperature or extending the oxidation time enhances the oxidation level of the nanomaterials. Oxygen-containing functional groups such as carboxyl, aldehyde, and phenolic groups can interact with carbon defect sites, enhancing surface reactivity, facilitating the deposition of metal NPs, and promoting surface wettability, which in turn promotes interfacial mass transfer.<sup>[41]</sup> This study offers novel insights into the conversion of biomass into catalyst supports and the promotion of metal catalyst loading, opening up new possibilities in this field.

## 2.5. Biomass for Metal Ion Reduction

In the past few decades, biomass nanomaterials have attracted significant attention in the domains of green chemistry and renewable energy. The inherent functional groups and distinctive biological structures found in biomass enable their effective utilization in the creation of sustainable nanomaterials for clean energy applications.<sup>[42]</sup> Extracts derived from plants, animals, or active organisms, encompassing substances like dopamine, aldose/ketose sugars, and polyphenols, can undergo bioreduction processes to form nanoscale structures that retain specific characteristics of the biomass's biological structure or functionality. These bio-derived nanomaterials offer advantages such as straightforward synthesis methods, low cost, and environmental compatibility. Extracts containing oxidizing and reducing groups can serve as reducing agents in redox reactions, enabling precise and controlled reduction of metal ions and facilitating large-scale synthesis. By harnessing the unique properties of biomass-based extracts, including their reducing capabilities and diverse functional groups, it becomes feasible to tailor the structures and properties of nanomaterials.<sup>[43]</sup> The integration of biomass-derived extracts and their redox properties presents a versatile platform for the development of sustainable and environmentally friendly nanomaterials across various applications.<sup>[44]</sup>

One of the primary objectives in nanotechnology is the development of simple and environmentally friendly synthesis methods that improve fabrication processes.<sup>[45]</sup> This entails precise control over cluster size and morphology, enabling large-scale production while minimizing potential pollution risks.<sup>[46]</sup> Iron oxide NPs possess diverse surface morphologies, unique nano-scale structures, and variable oxidation states, making them



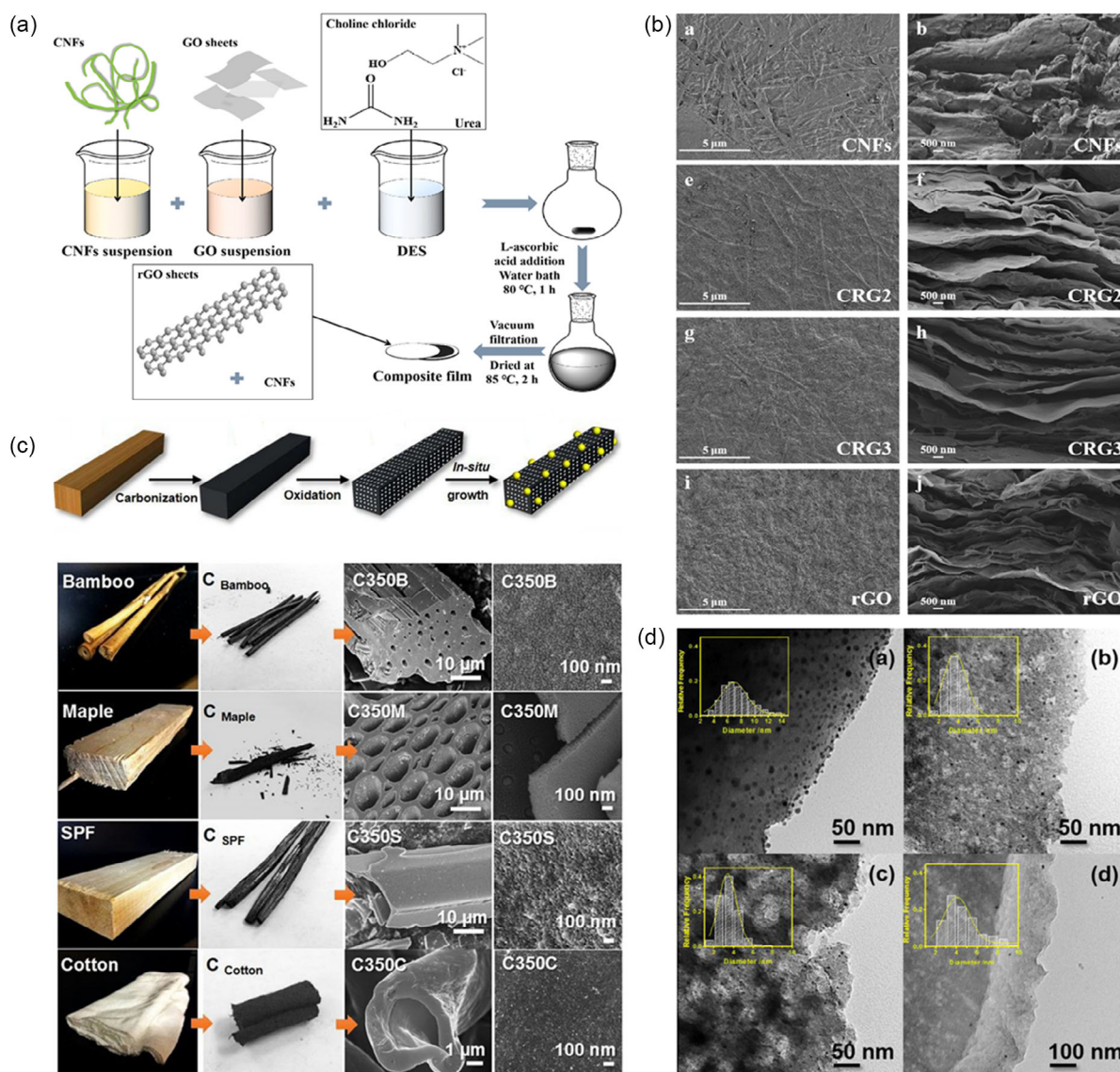


**Figure 5.** a) Schematic diagram of the preparation process of CNF/rGO composite film. b) Top side and cross-section SEM images of different materials. Reproduced with permission.<sup>[37]</sup> Copyright 2021, Elsevier. c) Schematic diagram of the preparation of porous carbon carriers, hybrid catalysts, as well as apparent images of biomass before carbonization and SEM images after carbonization. d) TEM and size distribution images of Ag loading of different carbonization precursors. Reproduced with permission.<sup>[40]</sup> Copyright 2016, Elsevier.

highly versatile in numerous fields. However, to retain their distinctive physicochemical properties, it is crucial to synthesize them under conditions that yield a narrow size distribution and monodispersity, preferably below 20 nm.<sup>[47]</sup> The utilization of red clover as a biofabrication method for the production of small metal particles under specific pH conditions holds significant promise. Suspensions of alfalfa were obtained by pretreatment such as grinding, washing, pH adjustment, and centrifugation. The alfalfa suspension was mixed with  $\text{FeNH}_4(\text{SO}_4)_2 \cdot 12\text{H}_2\text{O}$  aqueous solution and centrifuged to obtain iron oxide NPs with particle sizes below 5 nm (Figure 6a).<sup>[48]</sup> By further optimizing reaction conditions, including pH, even smaller NPs can be synthesized in a more controlled manner.

Additionally, the resulting NPs exhibit a face-centered cubic lattice, enhancing their stability at the quantum dot scale. The use of biomass for the production of small-sized NPs offers several advantages, including mild reaction conditions, controllable nanoparticle size and structure, and environmental friendliness. This approach provides novel insights into nanomaterial synthesis strategies.

Conventional techniques for removing heavy metal ions from wastewater, such as chemical precipitation, ion exchange, reverse osmosis, and electrochemical evaporation, often consume substantial energy.<sup>[49]</sup> Microorganisms, including fungi, have emerged as powerful tools for the removal of toxic heavy metal ions due to their small residual volume, rapid clearance rate, low



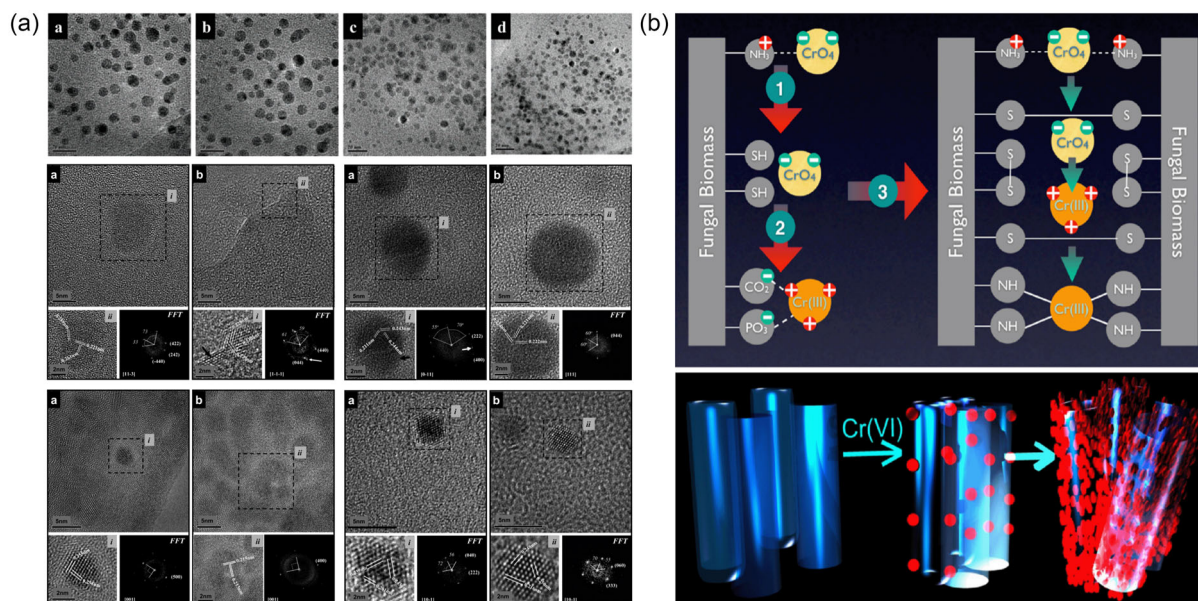


**Figure 6.** a) TEM and HRTEM images of samples prepared at different pH conditions. Reproduced with permission.<sup>[48]</sup> Copyright 2007, American Chemical Society. b) Possible reaction pathways of biomass surface functional groups interacting with metal ions. Reproduced with permission.<sup>[52]</sup> Copyright 2009, Elsevier.

cost, and widespread availability.<sup>[50]</sup> However, the practical application of live fungal cells with physiological activity is limited. Inactivated cells have thus become the preferred approach for metal ion reduction, offering advantages such as nontoxicity, absence of growth media requirements, and reusability.<sup>[51]</sup> Inactivated bacteria for heavy metal ion adsorption and reduction were obtained through natural drying, grinding, high-pressure thermal inactivation, and scrubbing. Through adsorption, coupling, and reduction processes using inactivated *Coriolus versicolor*, Cr<sup>6+</sup> can be transformed into Cr<sup>3+</sup> and subsequently released.<sup>[52]</sup> Carboxyl groups on the cell surface have been identified as the primary contributors to the adsorption capacity of Cr<sup>6+</sup>, while the fibrous framework composed of chitin provides numerous active sites. Additionally, the acetamide groups on the fibers can coordinate with metal ions (Figure 6b). Both thermal treatment and acidic pH conditions significantly enhance metal ion adsorption, with lower pH conditions favoring the reduction of Cr<sup>6+</sup>. This cost-effective, environmentally friendly, and efficient bioreduction method for metal ions offers new perspectives on reducing energy consumption, minimizing resource waste, and mitigating environmental pollution.

### 3. Applications of Biomass-Based Nanomaterials

#### 3.1. Biomass-Based Nanomaterials for Hydrogen Production

H<sub>2</sub> energy plays a pivotal role in reducing fossil fuel consumption and achieving sustainable development as a clean, nonpolluting, and renewable energy source.<sup>[53]</sup> Efficient photocatalytic hydrogen production relies on semiconductor catalysts that are nontoxic, stable, cost effective, and highly efficient. Among various hydrogen production technologies, solar-driven

photocatalytic H<sub>2</sub> production from wastewater holds great promise as a green energy source to replace fossil fuels.<sup>[54]</sup> In this context, nanostructured composites comprising biomass-activated carbon (AC) modified with Co<sub>3</sub>O<sub>4</sub> have been developed for photocatalytic H<sub>2</sub> production from H<sub>2</sub>S wastewater under solar irradiation (Figure 7a).<sup>[55]</sup> The hierarchical structure, high porosity, large specific surface area of Co<sub>3</sub>O<sub>4</sub>, and high conductivity of AC collectively contribute to the remarkable photocatalytic H<sub>2</sub> production performance of the Co<sub>3</sub>O<sub>4</sub>-AC nanocomposites. Under 730 W m<sup>-2</sup> solar irradiation, the H<sub>2</sub> yield of the Co<sub>3</sub>O<sub>4</sub>-AC nanocomposites is significantly higher compared to pristine Co<sub>3</sub>O<sub>4</sub> nanosheets, thanks to the synergistic effect between Co<sub>3</sub>O<sub>4</sub> and AC. Furthermore, as the concentration of sulfides and sulfites increases, the H<sub>2</sub> production rate reaches an impressive 70 mL h<sup>-1</sup>. However, excessive sulfide ions can inhibit the redox process, as the accumulation of sulfur species on the catalyst surface hinders the reaction. Additionally, the Co<sub>3</sub>O<sub>4</sub>-AC nanocomposites exhibit excellent cycling stability, a crucial factor for sustained photocatalytic H<sub>2</sub> production (Figure 7b). This study provides novel insights into green H<sub>2</sub> production through solar-driven wastewater treatment, opening up new avenues for sustainable energy generation.

In recent years, conjugated polymers have attracted considerable attention due to their unique nonmetallic structure, facile fabrication processes, and distinctive optical properties.<sup>[56]</sup> Among these polymers, graphitic carbon nitride (g-C<sub>3</sub>N<sub>4</sub>), composed of triazine units, has emerged as a prominent research focus in the field of photocatalytic water splitting for hydrogen production. This is attributed to its suitable bandgap, excellent cycling stability, and tunable electronic properties.<sup>[57]</sup> However, the photocatalytic performance of g-C<sub>3</sub>N<sub>4</sub> still falls short of expectations due to limited visible light absorption, fast recombination of electron-hole pairs, and limited active sites.<sup>[58]</sup>

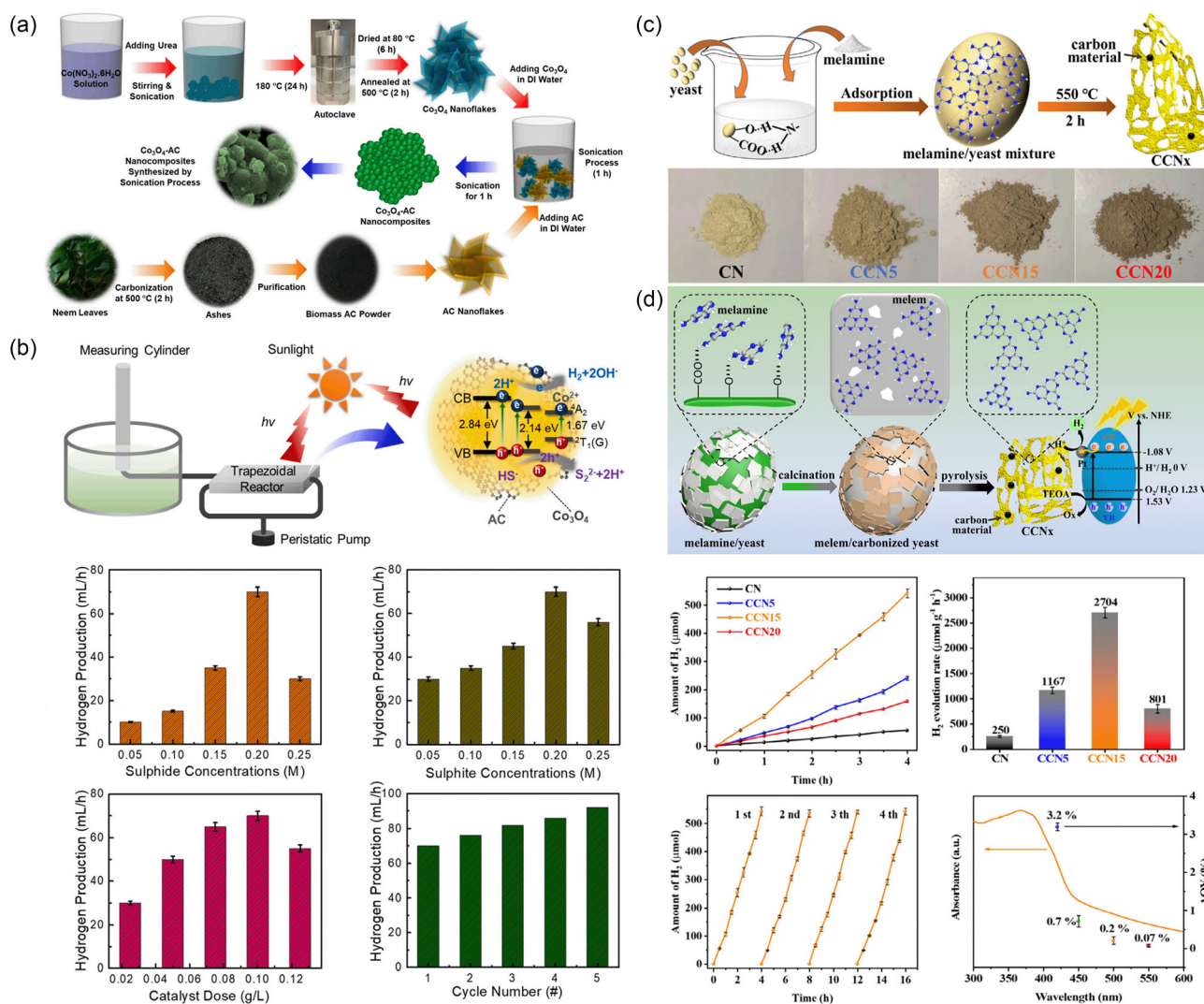


**Figure 7.** a) Schematic of the synthesis of Co<sub>3</sub>O<sub>4</sub>-AC nanocomposites. b) Photocatalytic H<sub>2</sub> production mechanism and performance characterization of Co<sub>3</sub>O<sub>4</sub>-AC nanocomposites. Reproduced with permission.<sup>[55]</sup> Copyright 2023, Elsevier. c) Schematic synthesis and apparent image of CCNx. d) Schematic diagram of material transformation process, photocatalytic mechanism, and performance evaluation. Reproduced with permission.<sup>[60]</sup> Copyright 2023, Elsevier.

Templates, acting as structural directing agents, are commonly employed to tailor the morphology and structure of photocatalysts. Biomass, as a cost-effective, diverse, and abundant resource, serves as an effective template for g-C<sub>3</sub>N<sub>4</sub> synthesis.<sup>[59]</sup> By polymerizing a melamine precursor on the surface of organic yeast, a biomass-derived graphitic carbon nitride with a thin-layered structure (CCNx) is prepared (Figure 7c).<sup>[60]</sup> The hydrogen bonding between melamine and yeast creates interface constraints, resulting in the formation of small-sized CCNx. CCNx exhibits enhanced visible light absorption, significantly improving the delocalization of electrons and facilitating the separation of photogenerated charge carriers. Under visible light irradiation, CCNx demonstrates a remarkable photocatalytic hydrogen evolution rate of 2704 μmol g<sup>-1</sup> h<sup>-1</sup>, nearly 11 times higher than that of pristine g-C<sub>3</sub>N<sub>4</sub>. Moreover, CCNx exhibits excellent cycling stability and resistance to photocorrosion after

multiple cycles (Figure 7d). This work harnesses the synergistic effects of morphology and composition control achieved through biomass templating, thereby offering broad prospects for the development of efficient nonmetallic photocatalysts.

### 3.2. Biomass-Based Nanomaterials for Carbon Dioxide Reduction

The accumulation of CO<sub>2</sub> poses a significant challenge to ecosystems, and achieving carbon neutrality has become a globally recognized goal.<sup>[61]</sup> Harnessing the abundance and low cost of CO<sub>2</sub> for its conversion into high-value chemicals represents an effective strategy to mitigate CO<sub>2</sub> accumulation and achieve energy and environmental sustainability.<sup>[62]</sup> Rice husks (RHs), composed of organic matter and silica dioxide, are abundant



biomass resources. Conventional approaches for converting RHs into photocatalysts often involve the combustion of organic matter, resulting in the release of large amounts of  $\text{CO}_2$ . However, the utilization of molten salt, an anaerobic high-temperature medium generated from the pyrolysis of organic matter, provides a unique avenue to accelerate the reduction of metal oxides by the generated carbon and facilitate metal functionalization.<sup>[63]</sup> Additionally, molten salt exhibits excellent in situ capture and conversion capabilities for  $\text{CO}_2$ , overcoming the interference of impurities in RHs and facilitating the self-purification process of biomass-derived photocatalysts.<sup>[64]</sup> Through the electrolysis of RHs and AgCl in molten salt, a SiC/C/Ag photocatalyst is constructed, demonstrating remarkable potential for  $\text{CO}_2$  reduction (Figure 8a).<sup>[65]</sup> Under light excitation, electrons are excited from the valence band (VB) of SiC to the conduction band (CB) and subsequently migrate to carbon, facilitating  $\text{CO}_2$  reduction. The incorporation of RHs and AgCl significantly reduces the energy consumption during catalyst preparation. The SiC/C/Ag photocatalyst exhibits significantly enhanced photocatalytic activity and a substantially reduced threshold for  $\text{CO}_2$  reduction. It demonstrates excellent photocurrent, high charge–hole pair separation

efficiency, rapid charge migration rate, and long carrier lifetime, enabling efficient photocatalytic reduction under visible light irradiation (Figure 8b). Notably, under simulated solar light irradiation, the photocatalytic  $\text{CO}_2$  reduction achieves CO and  $\text{CH}_4$  production rates of 48.0 and  $7.0 \mu\text{mol g}^{-1}$ , respectively. The apparent quantum efficiency of the photocatalyst at 365 nm reaches 0.32%, surpassing previous similar photocatalysts, while maintaining excellent stability. This work provides a promising approach for the preparation of  $\text{CO}_2$  reduction photocatalysts using biomass and molten salt, thereby contributing to the advancement of sustainable  $\text{CO}_2$  utilization strategies.

Plant photosynthesis harnesses solar energy to convert  $\text{CO}_2$ , providing a continuous and sustainable supply of renewable energy. This intricate process relies on a series of catalytic steps, including light absorption by chlorophyll, water splitting for oxygen evolution, NADPH generation, and  $\text{CO}_2$  fixation.<sup>[66]</sup> Inspired by natural photosynthesis, research in photocatalyst development and the construction of photocatalytic systems has made significant progress.<sup>[67]</sup> The integration of photocatalysis and biocatalysis requires establishing pathways for the transfer of reducing equivalents between these catalysts and creating compatible

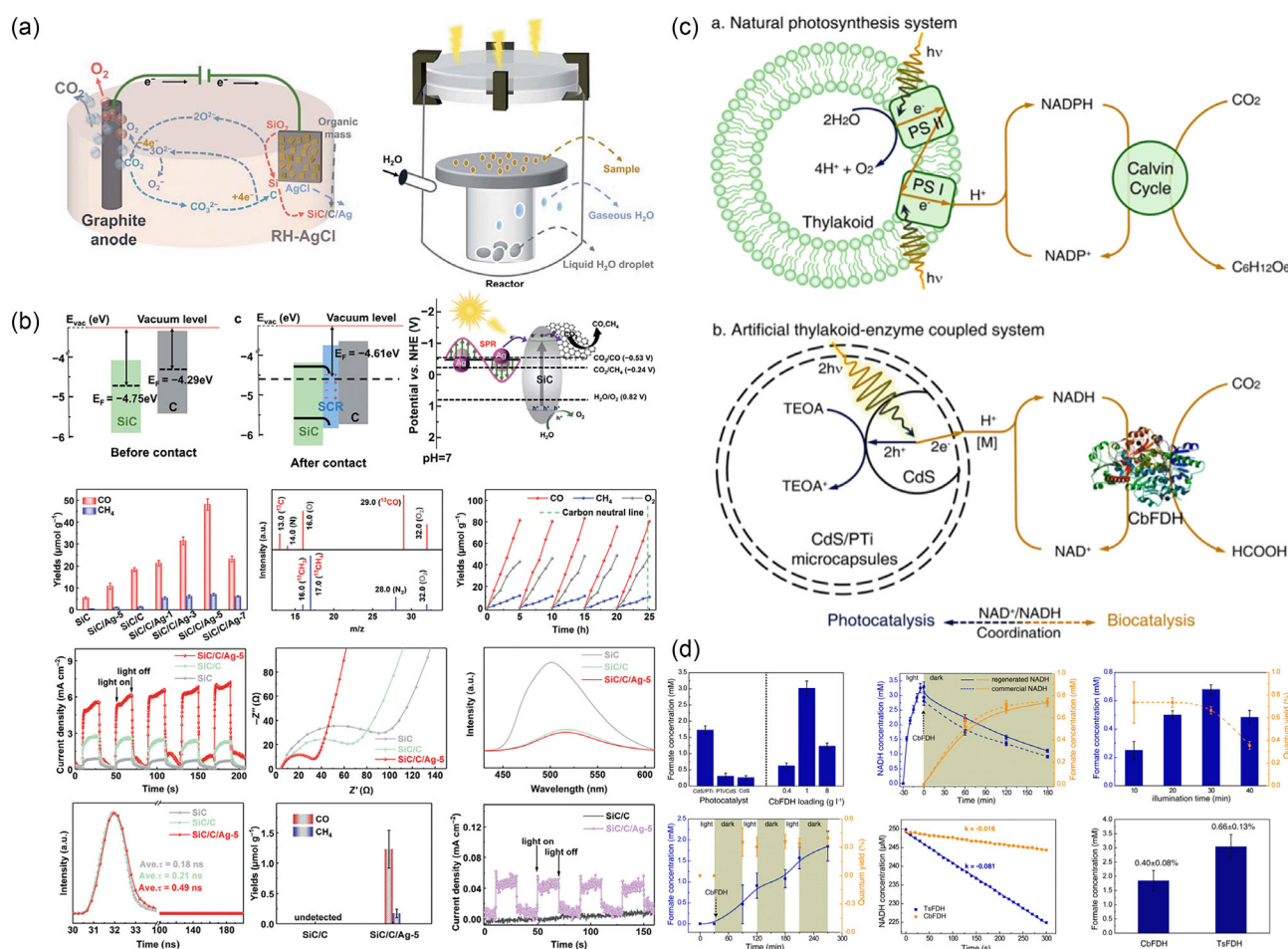


**Figure 8.** a) Schematic diagram of electrochemical conversion and device. b) Charge carrier migration mechanism and photocatalytic performance evaluation. Reproduced with permission.<sup>[65]</sup> Copyright 2021, Royal Society of Chemistry. c) Schematic of the similarity between natural photosynthesis and artificial vesicle-enzyme coupling system. d) Photocatalytic  $\text{CO}_2$  reduction performance test of microcapsules. Reproduced with permission.<sup>[70]</sup> Copyright 2019, American Chemical Society.



interfaces.<sup>[68]</sup> Currently, three representative artificial photosynthesis systems based on photocatalysis, photoelectrocatalysis, and photobiocatalysis have been developed for the continuous synthesis of fuels and chemicals.<sup>[69]</sup> Artificial photosynthesis holds great potential for the production of solar dyes and chemicals. Photobiocatalytic systems combine the light-harvesting ability of photocatalysts with the CO<sub>2</sub> reduction ability of biocatalysts, mimicking the biological prototype (Figure 8c). By modifying the inner wall of fish sperm protein-titanium dioxide (PTi) microcapsules with CdS quantum dots (QDs), an artificial vesicle is constructed for enzymatic and multi-enzymatic coupling of CO<sub>2</sub> reduction.<sup>[70]</sup> The vesicles spatially separate the photocatalytic and enzymatic reactions, preventing enzyme deactivation caused by photogenerated holes and reactive oxygen species (ROS), ensuring efficient compatibility between the two types of catalysts.<sup>[71]</sup> The heterostructure of CdS QDs and PTi facilitates the transfer of photoexcited electrons within the microcapsule, enabling the efficient regeneration of  $\beta$ -nicotinamide adenine dinucleotide (NADH) for subsequent enzymatic CO<sub>2</sub> reduction. The optimized system exhibits a NADH regeneration rate of  $4226 \pm 121 \mu\text{mol g}^{-1} \text{h}^{-1}$  and an optimal yield of  $93.03 \pm 3.84\%$ . This photobiocatalytic system enables the individual enzymes to produce formic acid and methanol at rates of 1500 and  $99 \mu\text{Mh}^{-1}$ , respectively (Figure 8d), paving the way for the construction of complex multireaction artificial catalytic systems. These advancements represent a significant step toward the realization of efficient and sustainable artificial photosynthesis.

### 3.3. Biomass-Based Nanomaterials for Batteries

Lithium-sulfur (Li-S) batteries have attracted significant interest due to their high energy density, environmental friendliness, cost-effectiveness, and the abundance of their raw materials.<sup>[72]</sup> However, Li-S batteries face formidable challenges, including volume expansion and the formation of polysulfide intermediates, resulting in poor rate performance, low coulombic efficiency, and limited cycling stability, which complicate their design and operation.<sup>[73]</sup> The changes in polarity, conductivity, and solubility of sulfur species further exacerbate these issues. Biological cells, with their selectively permeable membranes that regulate substance entry and exit, provide an excellent model for the design of Li-S batteries. Biomimetic bipolar microcapsules, fabricated through bacterial fermentation and chemical modification, can serve as microreactors to address the challenges faced by Li-S batteries (Figure 9a).<sup>[74]</sup> The nonpolar core of the biomimetic microcapsule is utilized for loading active materials, while the polar shell controls the selective transport of substances. The carbonaceous material inside the biomimetic microcapsule is derived through microbial fermentation and thermal treatment. Each microcapsule acts as a microreactor, adsorbing sulfur atoms on the porous carbon core, while the polar TiO<sub>2</sub> shell prevents the migration of polysulfides during lithium ion diffusion, effectively addressing the issue of poor cycling stability. The sulfur utilization in the biomimetic microcapsule cathode reaches 70.6%, effectively suppressing the migration of polysulfides during the cycling process. It can provide a specific capacity of  $1202 \text{ mAh g}^{-1}$  and exhibits a capacity decay rate of only

0.016% after 1500 cycles (Figure 9b). Through this biomimetic approach, waste microorganisms can be repurposed as cathode materials for sulfur batteries, further promoting the application of bio-synthesis technology in the field of batteries. These findings offer new insights into the design of Li-S batteries inspired by biological systems.

The depletion of fossil fuels and lithium resources necessitates the development of new energy storage technologies to enable the integration of renewable and clean energy sources.<sup>[75]</sup> Sodium-ion batteries (SIBs) have emerged as a promising alternative due to the abundance of sodium resources and their unique operating mechanism.<sup>[76]</sup> However, the further advancement and utilization of SIBs have been impeded by challenges associated with the larger size of sodium ions and the selection of suitable anode materials.<sup>[77]</sup> Traditional anode materials like graphite, alloys, and metal oxides are not well suited for SIBs due to issues such as thermodynamic limitations, narrow interlayer spacing, limited sodium storage capacity, and poor cycling stability.<sup>[78]</sup> Conversely, amorphous carbonaceous materials offer several advantages, including larger interlayer spacing and a higher density of structural defects, which provide ample diffusion pathways and abundant active adsorption sites for Na<sup>+</sup> ions, thereby enhancing sodium storage capacity. Carbonaceous materials derived from natural biomass possess favorable traits such as low cost and good stability, making them potential candidates for SIBs anode materials.<sup>[79]</sup>

Through a bottom-up pyrolysis process, carbonaceous materials can retain the structural characteristics of the biomass precursor while achieving uniform heteroatom doping, such as nitrogen, sulfur, and phosphorus. Carbon electrodes derived from waste silk protein exhibit increased interlayer spacing as a result of nitrogen doping, leading to the exposure of more active sites. Nitrogen sites act as negative centers, facilitating enhanced Na<sup>+</sup> adsorption.<sup>[80]</sup> The carbon electrode exhibits exceptional reversible discharge capacity even after 5000 cycles (Figure 9c). When assembled as an anode in SIBs after sodiation treatment, the full cell demonstrates a reversible discharge capacity of  $105.3 \text{ mAh g}^{-1}$ , high coulombic efficiency of 91.8%, and excellent cycling stability (Figure 9d). This study demonstrates the feasibility of commercial applications for all-SIBs using biomass-derived carbon rods as anode materials, offering promising prospects for the development of sustainable energy storage technologies.

### 3.4. Biomass-Based Nanomaterials for SCs

Micro-SCs (MSCs) have emerged as promising energy storage devices for smart electronic devices, offering high energy density, long cycle life, and rapid charge-discharge capabilities.<sup>[81]</sup> To overcome the electrochemical limitations of batteries, biomass has garnered significant attention in the development of sustainable energy storage systems. Biomass exhibits renewability, sustainability, structural flexibility, and chemical diversity, making it an attractive candidate for energy conduction and redox properties.<sup>[82]</sup> Fabricating MSCs using functional inks with suitable rheological properties for high-resolution screen printing is an effective approach. Pyrroloquinoline derivatives (PDs), which are key components of electron transfer proteins

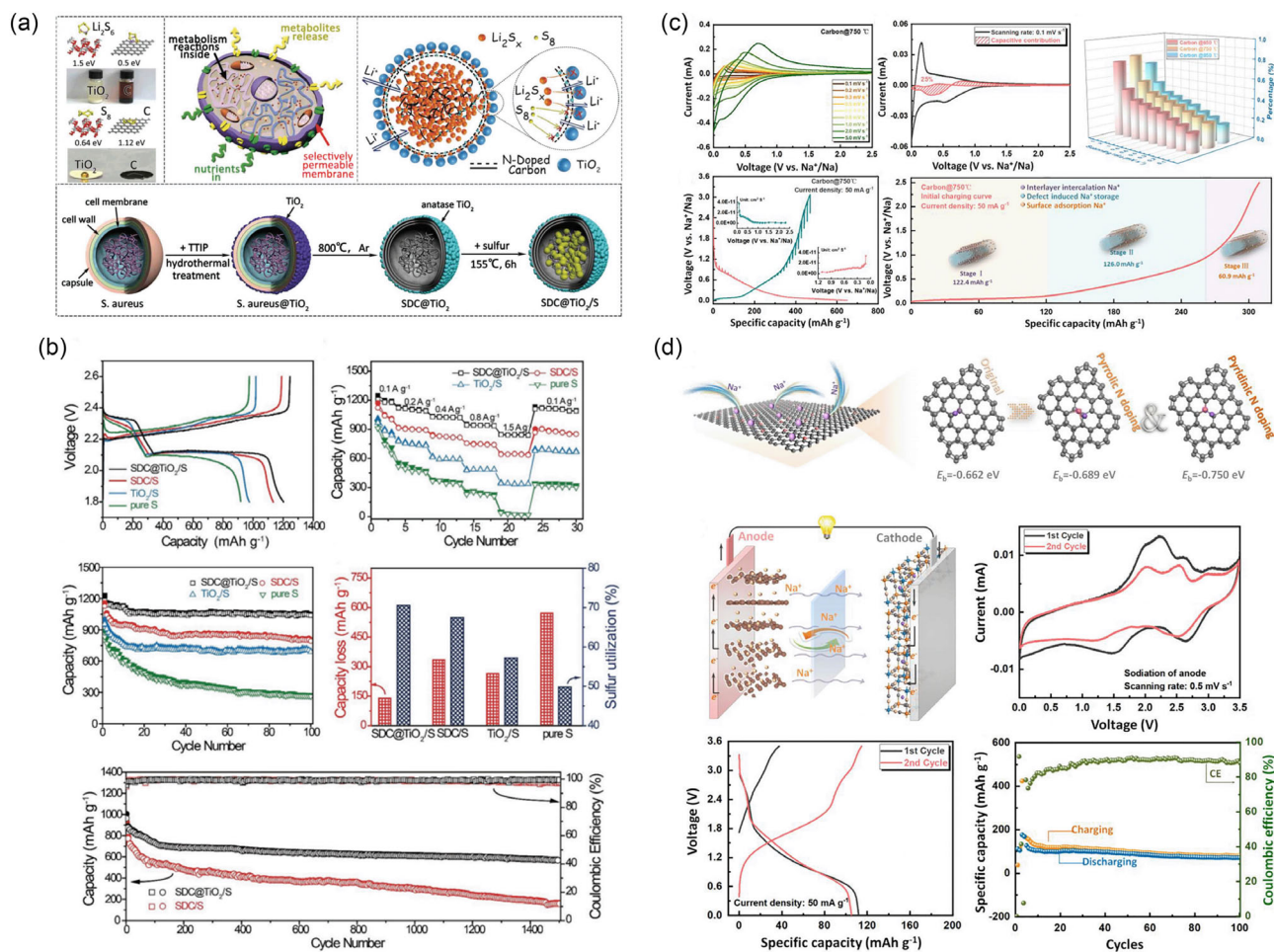


**Figure 9.** a) Schematic diagram of the design and synthesis process of biomass Li-S battery. b) Electrochemical characterization of biomass Li-S battery. Reproduced with permission.<sup>[74]</sup> Copyright 2018, Wiley-VCH. c) Electrochemical testing of carbonaceous nanorods for Na<sup>+</sup> battery and Na<sup>+</sup> storage mechanism. d) Schematic of the electrochemical device and electrochemical performance tests of the Na<sup>+</sup> full battery. Reproduced with permission.<sup>[80]</sup> Copyright 2021, Elsevier.

found in nature, possess a pyrroloquinoline quinone structure and high capacitance.

By coordinating PDs with biomass-derived porous graphene (BHG) through hydrogen bonding and  $\pi$ - $\pi$  stacking noncovalent interactions, biomass-based inks can be formulated (Figure 10a).<sup>[83]</sup> These inks enable scalable screen printing of flexible micro-SCs (FMSCs), allowing for the precise printing of diverse patterns and structures with high resolution. The printed MSCs exhibit an impressive capacitance of 95.3 mF cm<sup>-2</sup>, an energy density of 16.3  $\mu$ Wh cm<sup>-2</sup>, excellent cycling stability, and flexibility, rendering them suitable for applications in wearable devices and integrated electronics (Figure 10b). The noncovalent interactions between PDs as redox centers and BHG demonstrate that MSCs or FMSCs fabricated using stable screen-printing technology can serve as sustainable energy storage systems with broad prospects in the field of energy. This research paves the way for the development of biomass-based MSCs with enhanced performance and scalability, contributing to the advancement of sustainable energy storage technologies.

In recent years, with the growing demand for high-performance electronic devices and renewable energy sources, research related to novel energy storage devices has developed at a rapidly increasing rate.<sup>[84]</sup> Limited by factors such as poor structural utilization, biomass carbon aerogel (CA) suffers from undesirable energy density and specific capacitance problems, which seriously hinder its application in high performance.<sup>[85]</sup> The electrochemical performance of SCs depends on the performance of the electrode materials, and carbonaceous materials with different morphologies and sizes have been extensively studied as electrode materials for SCs. Although these carbonaceous materials provide better electrochemical performance for SCs, the obstacles of complicated preparation process, high cost, and unavoidable impact on the environment have greatly limited their conversion to commercial applications.<sup>[86]</sup> Binary composites with excellent electrochemical properties can be constructed by in situ growth of polypyrrole pseudocapacitor (PPy) particles on layered porous liquefied wood carbon aerogel (LWCA) (Figure 10c).<sup>[87]</sup> The deposition of PPy particles improves the energy density and specific capacitance of the SCs, and the

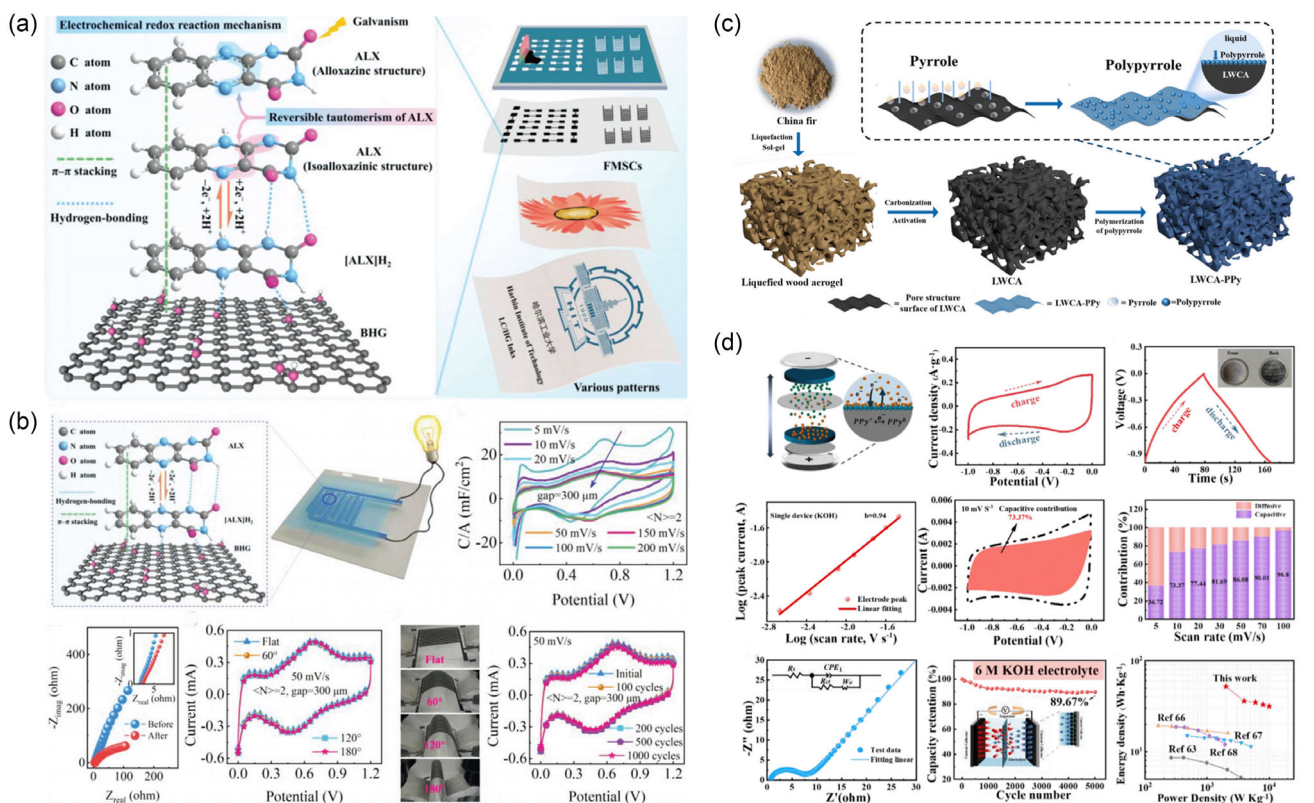


**Figure 10.** a) Schematic of FMSCs screen-printed using noncovalently interacting isoxazine/BHG inks. b) Energy storage mechanism and electrochemical characterization of printed-state MSCs. Reproduced with permission.<sup>[83]</sup> Copyright 2022, Wiley-VCH. c) Schematic of the synthesis of LWCA-PPy-x. d) Electrochemical characterization of LWCA-PPy-x in alkaline electrolyte. Reproduced with permission.<sup>[87]</sup> Copyright 2022, Elsevier.

layered structure of the LWCA can inhibit the aggregation of PPy particles while ensuring the rapid transfer of electrolyte ions. The assembled LWCA-PPy hybrid capacitive composites have a high capacitance performance of  $421.45 \text{ F g}^{-1}$  and excellent cycling stability. In the KOH electrolyte, the LWCA-PPy exhibited a remarkably energy density of  $52.0 \text{ Wh kg}^{-1}$  and power density of  $2012.8 \text{ W kg}^{-1}$  (Figure 10d). In the  $\text{H}_2\text{SO}_4$  electrolyte, LWCA-PPy still maintains excellent cycling performance. This 3D biomass composite aerogel exhibits excellent electrochemical properties and has a promising application in energy storage devices.

## 4. Conclusion and Perspectives

In this review, we summarized the research progress of biomass-based nanomaterials in the field of energy, including the design and preparation of biomass nanomaterials as well as their various applications in hydrogen production,  $\text{CO}_2$  reduction, and energy storage devices. Based on the current situation of environmental destruction caused by fossil energy consumption, there is a necessity to develop alternative energy resources that are renewable, sustainable, low cost, and environmentally. The preparation of high value-added nanomaterials from biomass is an effective way to dispose of biomass waste and provide green energy. The diverse morphological structures, elemental

compositions, and abundant functional groups of biomass make them important candidates for the preparation of carbonaceous nanomaterials and composites. However, due to the complex structure and composition of biomass precursors, the preparation of biomass-based nanomaterials with tunable physicochemical properties, highly compatible and complex reaction systems still present many challenges. In addition, biomass-based nanomaterials are currently in the laboratory stage, and there are technical barriers limiting their large-scale fabrication and quality management. Due to the diversity of surface groups, information on the critical active sites and mechanisms of interaction of biomass-based nanomaterials is still unclear. Furthermore, biomass-based nanomaterials suffer from suboptimal activity and instability. By combining biomass-based nanomaterials with functional components to construct composite nanosystems, the utilization of biomass can be improved while optimizing its catalytic properties. Through theoretical calculations and rational design, the reaction mechanism and synergistic effect between components of biomass-based nanomaterials and their composites can be further investigated, which will be conducive to further enhancement of their performance and economic efficiency. In addition, with the continuous development of machine learning, neural network algorithms, and artificial intelligence, applying them to guide the development and design of next-generation biomass-based nanomaterials can significantly broaden the species of biomass-based nanomaterials and the



types of catalytic substrates and effectively promote the process of their application and transformation in the energy field.

## Acknowledgements

Z.Y. and X.Z. contributed equally to this work. The work was supported by the Taishan Scholar Project of Shandong Province (tsqn202211168), the National Natural Science Foundation of China (52272212), the Natural Science Foundation of Shandong Province (ZR2022JQ20), and the Key Laboratory of Optic-electric Sensing and Analytical Chemistry for Life Science, MOE (M2022-7).

## Conflict of Interest

The authors declare no conflict of interest.

## Keywords

biomass, carbon sources, energy, nanomaterials, synthetic approaches

Received: July 17, 2023

Revised: September 5, 2023

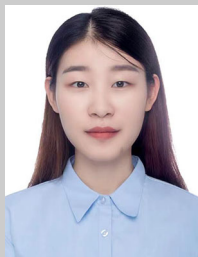
Published online:

- [1] a) Y. Xu, S. Li, M. Chen, J. Zhang, F. Rosei, *Trends Chem.* **2022**, *4*, 984; b) V. C. Hoang, M. Hassan, V. G. Gomes, *Appl. Mater. Today* **2018**, *12*, 342.
- [2] a) Z. Wang, D. Shen, C. Wu, S. Gu, *Green Chem.* **2018**, *20*, 5031; b) M. A. Cusenza, S. Longo, M. Cellura, F. Guarino, A. Messineo, M. Mistretta, M. Volpe, *Sustainable Prod. Consumption* **2021**, *28*, 866.
- [3] a) S. H. Lee, W. C. Lum, J. G. Boon, L. Kristak, P. Antov, M. Pędzik, T. Rogoziński, H. R. Taghiyari, M. A. R. Lubis, W. Fatriasari, S. M. Yadav, A. Chotikhun, A. Pizzi, *J. Mater. Res. Technol.* **2022**, *20*, 4630; b) J. M. Holmberg, L. Gustavsson, *Resour. Conserv. Recycl.* **2007**, *52*, 331.
- [4] a) Y. Liu, Y. Nie, X. Lu, X. Zhang, H. He, F. Pan, L. Zhou, X. Liu, X. Ji, S. Zhang, *Green Chem.* **2019**, *21*, 3499; b) E. J. Cho, L. T. P. Trinh, Y. Song, Y. G. Lee, H. J. Bae, *Bioresour. Technol.* **2020**, *298*, 122386.
- [5] S. Thanigaivel, S. Rajendran, L. Gnanasekaran, K. W. Chew, D. T. Tran, H.-D. Tran, N. K. Nghia, P. L. Show, *Environ. Chem. Lett.* **2023**, *21*, 821.
- [6] a) S. Babu, S. Singh Rathore, R. Singh, S. Kumar, V. K. Singh, S. K. Yadav, V. Yadav, R. Raj, D. Yadav, K. Shekhawat, O. Ali Wani, *Bioresour. Technol.* **2022**, *360*, 127566; b) M. Mujtaba, L. Fernandes Fraceto, M. Fazeli, S. Mukherjee, S. M. Savassa, G. Araujo de Medeiros, A. do Espírito Santo Pereira, S. D. Mancini, J. Lipponen, F. Vilaplana, *J. Cleaner Prod.* **2023**, *402*, 136815.
- [7] Y. Xie, K. S. Khoo, K. W. Chew, V. V. Devadas, S. J. Phang, H. R. Lim, S. Rajendran, P. L. Show, *Bioresour. Technol.* **2022**, *363*, 127830.
- [8] P. Zong, Y. Jiang, Y. Tian, J. Li, M. Yuan, Y. Ji, M. Chen, D. Li, Y. Qiao, *Energy Convers. Manage.* **2020**, *216*, 112777.
- [9] Z. Li, S. Wei, Y. Ge, Z. Zhang, Z. Li, *Sci. Total Environ.* **2023**, *858*, 160003.
- [10] a) F. Abnisa, W. M. A. Wan Daud, *Energy Convers. Manage.* **2014**, *87*, 71; b) M. K. Sah, S. Mukherjee, B. Flora, N. Malek, S. N. Rath, *J. Environ. Health Sci. Eng.* **2022**, *20*, 1015.
- [11] Z. Jiang, Z. Zhang, J. Liang, M. Zhou, D. Liu, D. Mao, Q. Zhang, W. Zhang, H. Li, L. Song, T. An, P. K. Wong, C. S. Lee, *Adv. Funct. Mater.* **2023**, *33*, 2301785.
- [12] a) V. G. Matveeva, L. M. Bronstein, *Prog. Mater. Sci.* **2022**, *130*, 100999; b) J. Popp, S. Kovacs, J. Olah, Z. Diveki, E. Balazs, *New Biotechnol.* **2021**, *60*, 76.
- [13] a) A. A. Melaibari, A. S. Elamoudi, M. E. Mostafa, N. H. Abu-Hamdeh, *Eng. Anal. Boundary Elem.* **2023**, *147*, 164; b) L. Chen, G. Msigwa, M. Yang, A. I. Osman, S. Fawzy, D. W. Rooney, P. S. Yap, *Environ. Chem. Lett.* **2022**, *20*, 2277; c) L. G. Kemeny, *Math. Comput. Simul.* **1982**, *24*, 194.
- [14] a) H. E. Karahan, M. Ji, J. L. Pinilla, X. Han, A. Mohamed, L. Wang, Y. Wang, S. Zhai, A. Montoya, H. Beyenal, Y. Chen, *J. Mater. Chem. B* **2020**, *8*, 9668; b) J. Huang, J. Liu, J. Wang, *Trac-Trend Anal. Chem.* **2020**, *124*, 115800.
- [15] B. Ates, S. Koytepe, A. Ulu, C. Gurses, V. K. Thakur, *Chem. Rev.* **2020**, *120*, 9304.
- [16] W. J. Liu, H. Jiang, H. Q. Yu, *Chem. Rev.* **2015**, *115*, 12251.
- [17] a) J. Abraham, K. S. Vasu, C. D. Williams, K. Gopinadhan, Y. Su, C. T. Cherian, J. Dix, E. Prestat, S. J. Haigh, I. V. Grigorieva, P. Carbone, A. K. Geim, R. R. Nair, *Nat. Nanotechnol.* **2017**, *12*, 546; b) L. Yu, C. Shearer, J. Shapter, *Chem. Rev.* **2016**, *116*, 13413.
- [18] S. Zhang, S.-F. Jiang, B.-C. Huang, X.-C. Shen, W.-J. Chen, T.-P. Zhou, H.-Y. Cheng, B.-H. Cheng, C.-Z. Wu, W.-W. Li, H. Jiang, H.-Q. Yu, *Nat. Sustainability* **2020**, *3*, 753.
- [19] J. Mao, J. Iocozzia, J. Huang, K. Meng, Y. Lai, Z. Lin, *Energy Environ. Sci.* **2018**, *11*, 772.
- [20] a) N. Hüsing, U. Schubert, *Angew. Chem. Int. Ed.* **1998**, *37*, 22; b) X. Lu, M. C. Arduini-Schuster, J. Kuhn, O. Nilsson, J. Fricke, R. W. Pekala, *Science* **1992**, *255*, 971.
- [21] H.-J. Zhan, K.-J. Wu, Y.-L. Hu, J.-W. Liu, H. Li, X. Guo, J. Xu, Y. Yang, Z.-L. Yu, H.-L. Gao, X.-S. Luo, J.-F. Chen, Y. Ni, S.-H. Yu, *Chem* **2019**, *5*, 1871.
- [22] C. Li, Y. W. Ding, B. C. Hu, Z. Y. Wu, H. L. Gao, H. W. Liang, J. F. Chen, S. H. Yu, *Adv. Mater.* **2020**, *32*, e1904331.
- [23] B. C. Hu, H. R. Zhang, S. C. Li, W. S. Chen, Z. Y. Wu, H. W. Liang, H. P. Yu, S. H. Yu, *Adv. Funct. Mater.* **2022**, *33*, 2207532.
- [24] a) S. Miao, K. Liang, J. Zhu, B. Yang, D. Zhao, B. Kong, *Nano Today* **2020**, *33*, 100879; b) J. Wang, S. Kaskel, *J. Mater. Chem.* **2012**, *22*, 23710.
- [25] P. Akbarzadeh, N. Koukabi, *Appl. Organomet. Chem.* **2021**, *35*, e6039.
- [26] B. Han, C. E. Carlton, A. Kongkanand, R. S. Kukreja, B. R. Theobald, L. Gan, R. O'Malley, P. Strasser, F. T. Wagner, Y. Shao-Horn, *Energy Environ. Sci.* **2015**, *8*, 258.
- [27] Z.-Y. Sui, X. Li, Z.-Y. Sun, H.-C. Tao, P.-Y. Zhang, L. Zhao, B.-H. Han, *Carbon* **2018**, *126*, 111.
- [28] a) C. Guo, W. Liao, Z. Li, L. Sun, C. Chen, *Nanoscale* **2015**, *7*, 15990; b) J. J. Lv, Y. Li, S. Wu, H. Fang, L. L. Li, R. B. Song, J. Ma, J. J. Zhu, *ACS Appl. Mater. Interfaces* **2018**, *10*, 11678.
- [29] L. Li, Z. Wu, J. Zhang, Y. Zhao, G. Shao, *ChemElectroChem* **2021**, *8*, 4790.
- [30] H. W. Shim, Y. H. Jin, S. D. Seo, S. H. Lee, D. W. Kim, *ACS Nano* **2011**, *5*, 443.
- [31] X. Yu, X. Jin, X. Chen, A. Wang, J. Zhang, J. Zhang, Z. Zhao, M. Gao, L. Razzari, H. Liu, *ACS Nano* **2020**, *14*, 13876.
- [32] H.-W. Shim, A.-H. Lim, K.-M. Min, D.-W. Kim, *CrystEngComm* **2011**, *13*, 6747.
- [33] S. Cui, N. Song, L. Shi, P. Ding, *ACS Sustainable Chem. Eng.* **2020**, *8*, 6363.
- [34] R. Guo, L. Zhang, Y. Lu, X. Zhang, D. Yang, *J. Energy Chem.* **2020**, *51*, 342.
- [35] a) D. Trache, V. K. Thakur, R. Boukherroub, *Nanomaterials* **2020**, *10*, 1523; b) O. P. Troncoso, F. G. Torres, *Int. J. Mol. Sci.* **2020**, *21*, 6532.
- [36] A. A. M. Elgharabawy, M. Hayyan, A. Hayyan, W. J. Basirun, H. M. Salleh, M. E. S. Mirghani, *Biomass Bioenergy* **2020**, *137*, 105550.

- [37] Q. Liu, W. Sun, T. Yuan, S. B. Liang, F. Peng, C. L. Yao, *Carbohydr. Polym.* **2021**, 272, 118514.
- [38] A. Jain, R. Balasubramanian, M. P. Srinivasan, *Chem. Eng. J.* **2016**, 283, 789.
- [39] L. Chen, T. Ji, L. Brisbin, J. Zhu, *ACS Appl. Mater. Interfaces* **2015**, 7, 12230.
- [40] T. Ji, L. Chen, L. Mu, R. Yuan, M. Knoblauch, F. S. Bao, Y. Shi, H. Wang, J. Zhu, *Chem. Eng. J.* **2016**, 295, 301.
- [41] A. Kuznetsova, I. Popova, J. T. Yates Jr., M. J. Bronikowski, C. B. Huffman, J. Liu, R. E. Smalley, H. H. Hwu, J. G. Chen, *J. Am. Chem. Soc.* **2001**, 123, 10699.
- [42] Y. Feng, J. Jiang, Y. Xu, S. Wang, W. An, Q. Chai, U. H. Prova, C. Wang, G. Huang, *Carbon* **2023**, 211, 118105.
- [43] R. G. Haverkamp, A. T. Marshall, *J. Nanopart. Res.* **2008**, 11, 1453.
- [44] V. Kumar, S. K. Yadav, *J. Chem. Technol. Biotechnol.* **2009**, 84, 151.
- [45] S. Bognár, P. Putnik, D. Šojić Merkulov, *Nanomaterials* **2022**, 12, 263.
- [46] P. L. Saldanha, V. Lesnyak, L. Manna, *Nano Today* **2017**, 12, 46.
- [47] a) M. Benz, A. M. van der Kraan, R. Prins, *Appl. Catal., A* **1998**, 172, 149; b) Y. Zhang, N. Kohler, M. Zhang, *Biomaterials* **2002**, 23, 1553.
- [48] R. Herrera-Becerra, C. Zorrilla, J. A. Ascencio, *J. Phys. Chem. C* **2007**, 111, 16147.
- [49] S. Rengaraj, K. H. Yeon, S. H. Moon, *J. Hazard. Mater.* **2001**, 87, 273.
- [50] . Priyanka, S. K. Dwivedi, *J. Water Process Eng.* **2023**, 53, 103800.
- [51] L. Velasquez, J. Dussan, *J. Hazard. Mater.* **2009**, 167, 713.
- [52] R. Sanghi, N. Sankaramakrishnan, B. C. Dave, *J. Hazard. Mater.* **2009**, 169, 1074.
- [53] J. A. Turner, *Science* **2004**, 305, 972.
- [54] a) H. Nishiyama, T. Yamada, M. Nakabayashi, Y. Maehara, M. Yamaguchi, Y. Kuromiya, Y. Nagatsuma, H. Tokudome, S. Akiyama, T. Watanabe, R. Narushima, S. Okunaka, N. Shibata, T. Takata, T. Hisatomi, K. Domen, *Nature* **2021**, 598, 304; b) Y. Zhang, J. Zhao, H. Wang, B. Xiao, W. Zhang, X. Zhao, T. Lv, M. Thangamuthu, J. Zhang, Y. Guo, J. Ma, L. Lin, J. Tang, R. Huang, Q. Liu, *Nat. Commun.* **2022**, 13, 58.
- [55] J. Hu, X. Li, J. Qu, X. Yang, Y. Cai, T. Yang, F. Yang, C. M. Li, *Chem. Eng. J.* **2023**, 453, 139957.
- [56] X. Hu, Z. Zhan, J. Zhang, I. Hussain, B. Tan, *Nat. Commun.* **2021**, 12, 6596.
- [57] a) G. Liao, Y. Gong, L. Zhang, H. Gao, G.-J. Yang, B. Fang, *Energy Environ. Sci.* **2019**, 12, 2080; b) X. Wang, K. Maeda, A. Thomas, K. Takanabe, G. Xin, J. M. Carlsson, K. Domen, M. Antonietti, *Nat. Mater.* **2009**, 8, 76.
- [58] A. Wang, C. Wang, L. Fu, W. Wong-Ng, Y. Lan, *Nano-Micro Lett.* **2017**, 9, 47.
- [59] M. A. Mohamed, M. F. M. Zain, L. Jeffery Minggu, M. B. Kassim, N. A. Saidina Amin, W. N. W. Salleh, M. N. I. Salehmin, M. F. Md Nasir, Z. A. Mohd Hir, *Appl. Catal., B* **2018**, 236, 265.
- [60] L. Lei, H. Fan, Y. Jia, X. Wu, N. Hu, Q. Zhong, W. Wang, *J. Colloid Interface Sci.* **2023**, 634, 1014.
- [61] a) A. M. Appel, J. E. Bercaw, A. B. Bocarsly, H. Dobbek, D. L. DuBois, M. Dupuis, J. G. Ferry, E. Fujita, R. Hille, P. J. Kenis, C. A. Kerfeld, R. H. Morris, C. H. Peden, A. R. Portis, S. W. Ragsdale, T. B. Rauchfuss, J. N. Reek, L. C. Seefeldt, R. K. Thauer, G. L. Waldrop, *Chem. Rev.* **2013**, 113, 6621; b) Z. J. Wang, H. Song, H. Liu, J. Ye, *Angew. Chem. Int. Ed.* **2020**, 59, 8016.
- [62] S. Liu, M. Wang, Q. Cheng, Y. He, J. Ni, J. Liu, C. Yan, T. Qian, *ACS Nano* **2022**, 16, 17911.
- [63] W. Weng, J. Zhou, D. Gu, W. Xiao, *J. Mater. Chem. A* **2020**, 8, 4800.
- [64] D. Pang, W. Weng, J. Zhou, D. Gu, W. Xiao, *J. Energy Chem.* **2021**, 55, 102.
- [65] J. Wang, J. Xiao, Y. Shen, X. Liang, T. Lv, W. Xiao, *J. Mater. Chem. A* **2021**, 9, 27442.
- [66] a) Q. Li, R. Liu, Z. Li, H. Fan, J. Song, *Plant Physiol. Biochem.* **2022**, 177, 32; b) G. A. Karlin-Neumann, E. M. Tobin, *EMBO J.* **1986**, 5, 9.
- [67] J. L. White, M. F. Baruch, J. E. Pander Iii, Y. Hu, I. C. Fortmeyer, J. E. Park, T. Zhang, K. Liao, J. Gu, Y. Yan, T. W. Shaw, E. Abelev, A. B. Bocarsly, *Chem. Rev.* **2015**, 115, 12888.
- [68] K. K. Sakimoto, N. Kornienko, S. Cestellos-Blanco, J. Lim, C. Liu, P. Yang, *J. Am. Chem. Soc.* **2018**, 140, 1978.
- [69] a) N. S. Lewis, *Nat. Nanotechnol.* **2016**, 11, 1010; b) N. Kornienko, J. Z. Zhang, K. K. Sakimoto, P. Yang, E. Reisner, *Nat. Nanotechnol.* **2018**, 13, 890.
- [70] S. Zhang, J. Shi, Y. Sun, Y. Wu, Y. Zhang, Z. Cai, Y. Chen, C. You, P. Han, Z. Jiang, *ACS Catal.* **2019**, 9, 3913.
- [71] J. F. Allen, W. B. de Paula, S. Puthiyaveetil, J. Nield, *Trends Plant Sci.* **2011**, 16, 645.
- [72] T. D. Bogart, D. Oka, X. Lu, M. Gu, C. Wang, B. A. Korgel, *ACS Nano* **2014**, 8, 915.
- [73] a) P. P. R. M. L. Harks, C. B. Robledo, T. W. Verhallen, P. H. L. Notten, F. M. Mulder, *Adv. Energy Mater.* **2017**, 7, 1601635; b) A. Manthiram, Y. Fu, Y. S. Su, *Acc. Chem. Res.* **2013**, 46, 1125.
- [74] W. Wu, J. Pu, J. Wang, Z. Shen, H. Tang, Z. Deng, X. Tao, F. Pan, H. Zhang, *Adv. Energy Mater.* **2018**, 8, 1702373.
- [75] X. Ji, *Energy Environ. Sci.* **2019**, 12, 3203.
- [76] J. Y. Hwang, S. T. Myung, Y. K. Sun, *Chem. Soc. Rev.* **2017**, 46, 3529.
- [77] J. Sun, W. Tu, C. Chen, A. Plewa, H. Ye, J. A. Sam Oh, L. He, T. Wu, K. Zeng, L. Lu, *Chem. Mater.* **2019**, 31, 7311.
- [78] a) M. M. Doeff, Y. Ma, S. J. Visco, L. C. De Jonghe, *J. Electrochem. Soc.* **2019**, 140, L169; b) T. Chen, W. Liu, Y. Zhuo, H. Hu, M. Zhu, R. Cai, X. Chen, J. Yan, K. Liu, *J. Energy Chem.* **2020**, 43, 148.
- [79] J. Zhu, J. Roscow, S. Chandrasekaran, L. Deng, P. Zhang, T. He, K. Wang, L. Huang, *ChemSusChem* **2020**, 13, 1275.
- [80] J. Sun, Y. Sun, J. A. S. Oh, Q. Gu, W. Zheng, M. Goh, K. Zeng, Y. Cheng, L. Lu, *J. Energy Chem.* **2021**, 62, 497.
- [81] a) D. P. Dubal, N. R. Chodankar, D. H. Kim, P. Gomez-Romero, *Chem. Soc. Rev.* **2018**, 47, 2065; b) J. Liang, Y. Feng, L. Liu, S. Li, C. Jiang, W. Wu, *J. Mater. Chem. A* **2019**, 7, 15960.
- [82] a) K. Lin, R. Gómez-Bombarelli, E. S. Beh, L. Tong, Q. Chen, A. Valle, A. Aspuru-Guzik, M. J. Aziz, R. G. Gordon, *Nat. Energy* **2016**, 1, 16102; b) J. Hong, M. Lee, B. Lee, D. H. Seo, C. B. Park, K. Kang, *Nat. Commun.* **2014**, 5, 5335.
- [83] T. Wang, W. Yu, D. Wu, W. Zhao, M. Wang, J. Xu, J. Zhang, *Adv. Funct. Mater.* **2023**, 33, 2301896.
- [84] a) J. Cheng, S.-C. Hu, G.-T. Sun, K. Kang, M.-Q. Zhu, Z.-C. Geng, *Energy* **2021**, 215, 119144; b) Y. Liu, X. Xu, Y. Wei, Y. Chen, M. Gao, Z. Zhang, C. Si, H. Li, X. Ji, J. Liang, *Nano Lett.* **2022**, 22, 3784.
- [85] G. A. Tafete, M. K. Abera, G. Thothadri, *J. Energy Storage* **2022**, 48, 103938.
- [86] C. Zheng, W. Qian, C. Cui, G. Xu, M. Zhao, G. Tian, F. Wei, *J. Nat. Gas. Chem.* **2012**, 21, 233.
- [87] C. Lv, X. Ma, R. Guo, D. Li, X. Hua, T. Jiang, H. Li, Y. Liu, *Energy* **2023**, 270, 126830.



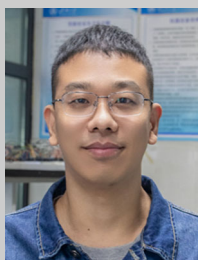
**Zhongwei Yang** obtained his B.E. degree in materials chemistry from Yantai University in 2020 and M.S. degree in physical chemistry from University of Jinan in 2023. Currently, he is working as a research assistant in Prof. Xin Yu's group at Institute for Advanced Interdisciplinary Research (iAIR). His research interests focus on the design and synthesis of nanomaterials for catalysis, energy, and biomedical applications.



**Xiaoyu Zhang** is currently a graduate student at the School of Chemistry and Chemical Engineering at University of Jinan in China. She received bachelor's degree in 2021 from Shandong Normal University in China. She is studying in Prof. Xin Yu's group at Institute for Advanced Interdisciplinary Research (iAIR). Her current research interest is the photocatalytic and enzymatic antibacterial therapy of layered double hydroxides (LDH).



**Hong Liu** is a professor in Shandong University and University of Jinan, China. He received his PhD degree in 2001 from Shandong University. His current research interest focuses on tissue engineering and stem cells, biosensors, photo-electrical functional materials. He has published more than 400 papers with total citation of over 36000 and H-index of 86. In 2009, he was awarded as Distinguished Young Scholar by National Natural Science Foundation of China. He was included in the Clarivate Analytics' Highly Cited Researchers 2018-2022 list. In 2022, as editor-in-chief, he launched a new journal, BMEMat (<https://onlinelibrary.wiley.com/journal/27517446>).



**Xin Yu** received his Ph.D. degree from Beijing Institute of Nanoenergy and Nanosystems, Chinese Academy of Sciences in 2017. Now he is a professor at Institute for Advanced Interdisciplinary Research, University of Jinan, Shandong. His current research mainly focused on the design and synthesis of nanomaterials and functional crystals and their applications for environment, energy, biological diagnosis, and therapy. He has published more than 80 papers with total citation of over 3500 and H-index of 32.